ORIGINAL ARTICLE

European Journal of Haematology WILEY

Idiopathic multicentric Castleman disease with marrow fibrosis and extramedullary hematopoiesis

Marley Blommers[1] | Sorin Selegean[2] | Richard K. Wood[2] |
Mateo Sarmiento Bustamante[3] | Saishravan Shyamsundar[3] | E. Ashley Wiley[4] |
Emilie Comeau[5] | Allam A. Shawwa[2] | Stefan Rose-John[6] |
David C. Fajgenbaum[3] | Luke Y. C. Chen[5,7]

[1]Faculty of Medicine, Dalhousie University, Halifax, Nova Scotia, Canada

[2]Department of Pathology, Dalhousie University

[3]Center for Cytokine Storm Treatment & Laboratory, Department of Medicine, Perelman School of Medicine, University of Pennsylvania, Philadelphia, Pennsylvania, USA

[4]Department of Diagnostic Radiology, Dalhousie University, Halifax, Nova Scotia, Canada

[5]Division of Hematology, Dalhousie University, Halifax, Nova Scotia, Canada

[6]Biochemical Institute, Medical Faculty, Christian-Albrechts-University, Kiel, Germany

[7]Division of Hematology, University of British Columbia, Vancouver, British Columbia, Canada

Correspondence
David C. Fajgenbaum, University of Pennsylvania, Perelman School of Medicine, Division of Translational Medicine & Human Genetics, Center for Cytokine Storm Treatment & Laboratory (CSTL), 3535 Market Street, Suite 700, Room 717, Philadelphia, PA 19104, USA.
Email: davidfa@pennmedicine.upenn.edu

Luke Y. C. Chen, Dalhousie University, Faculty of Medicine, Division of Hematology, 276 South Park Street, Suite 416 Bethune Building, Halifax, Nova Scotia, B3H 2Y9, Canada.
Email: lchen2@bccancer.bc.ca

Abstract

Background: Idiopathic multicentric Castleman disease (iMCD) is a rare inflammatory disorder mediated by excessive proinflammatory cytokine signaling, most notably by interleukin 6 (IL-6). IL-6-induced extramedullary hematopoiesis (EMH) has been reported in murine models of iMCD. Herein we present four cases of iMCD with EMH in humans.

Case Series: The index case is a 24-year-old white woman who presented with pancytopenia, hepatosplenomegaly, and diffuse lymphadenopathy (LAD) with EMH in core lymph node biopsies. We then searched ACCELERATE, a Castleman disease (CD) natural history registry, and identified three additional CD cases with EMH reported in biopsies: A 23-year-old Asian man with fatigue, edema, LAD, and splenomegaly; a 20-year-old white man with fever, dyspnea, LAD, and hepatosplenomegaly; and a 50-year-old white man with constitutional symptoms, LAD, and myelodysplastic syndrome in bone marrow with a KRAS mutation.

Results: All four patients presented with thrombocytopenia and fever and/or markedly elevated C-reactive protein. Patient 1 had iMCD-NOS (not otherwise specified) with severe thrombocytopenia, reticulin fibrosis in bone marrow, small volume LAD and organomegaly but no anasarca. The other three patients had iMCD-TAFRO (thrombocytopenia, anasarca, reticulin fibrosis, renal dysfunction, organomegaly). Two had mixed CD and two had hypervascular CD in lymph nodes. All four had bone

marrow hypercellularity and megakaryocyte hyperplasia and two had reticulin fibrosis.

Conclusions: This case series demonstrates that EMH can be seen in CD, particularly in iMCD-TAFRO. Given the similarity of this finding to previous murine models of IL-6-induced marrow and lymph node changes we hypothesize that this is an IL-6-mediated phenomenon.

KEYWORDS
Castleman disease, extramedullary hematopoiesis, IL-6, lymphadenopathy

Novelty Statement

What is the NEW aspect of your work? (One sentence)
The case series is the first to describe extramedullary hematopoiesis (EMH) in human patients with idiopathic multicentric Castleman disease (iMCD), paralleling findings of murine models of CD and suggesting a role for IL-6 signaling.

What is the CENTRAL finding of your work? (One sentence)
EMH can be seen in the lymph nodes of patients with iMCD who have thrombocytopenia, small volume lymphadenopathy, and severe inflammation.

What is (or could be) the SPECIFIC clinical relevance of your work? (One sentence)
This finding justifies further research into the pathophysiology of Castleman-like changes in lymph nodes.

1 | INTRODUCTION

Human herpes virus 8 negative idiopathic multicentric Castleman disease (HHV-8 negative iMCD) is a rare inflammatory lymphoproliferative disorder of unknown etiology.[1,2] HHV-8 negative iMCD is divided into three clinical subtypes: iMCD-TAFRO (thrombocytopenia, anasarca, fever, reticulin myelofibrosis or renal dysfunction, and organomegaly), iMCD-IPL (idiopathic plasmacytic lymphadenopathy), and iMCD-NOS (not otherwise specified).[3,4] Clinically, all MCD subtypes share some characteristic features: systemic inflammatory symptoms, generalized lymphadenopathy, laboratory abnormalities, and organ system dysfunction.[5] The most aggressive subtype is iMCD-TAFRO, which typically presents with acute onset and severe illness characterized by thrombocytopenia, minor lymphadenopathy and reticulin fibrosis in bone marrow,[4] and often with adrenalitis or adrenal hemorrhage as well.[6] Diagnosis of iMCD-TAFRO requires fulfillment of three major clinical criteria (thrombocytopenia, anasarca, and fever or systemic inflammation) and at least two of four minor categories.[7] The other two subtypes, iMCD-NOS and iMCD-IPL, have a less aggressive clinical course with the latter typically presenting with anemia, fatigue, polyclonal hypergammaglobulinemia, thrombocytosis, and elevated C-reactive protein (CRP) levels.[4,8]

Histologically, there are three types of pathological iMCD variants: hypervascular (HV), plasma cell (PC), and "mixed."[1,9] Lymph nodes with HV histopathology are characterized by capsular fibrosis, increased number of lymphoid follicles with regressed germinal centers, often >1 within the same mantle zone.[10,11] Lymph nodes exhibiting PC histopathology have hyperplastic germinal centers with distinct sheets of PCs in the interfollicular zone.[10,12] Nodes manifesting both HV and PC characteristics are classified as mixed variant. The HV pattern predominantly presents in patients with iMCD-TAFRO, whereas PC and mixed variants are more frequently observed in iMCD-IPL and iMCD-NOS cases.[13]

Although the pathophysiology of iMCD remains not fully understood, the proinflammatory cytokine interleukin-6 (IL-6) is both a central driver of disease pathogenesis and a key therapeutic target. Specifically, IL-6 levels exhibit a positive correlation with disease symptomology, and inhibition of IL-6 serves as the recommended first-line treatment for iMCD.[14] Mice infected with IL-6-expressing recombinant retrovirus recapitulate many features of iMCD, including anemia, splenomegaly, peripheral lymphadenopathy, hypoalbuminemia, and transient granulocytosis.[15] In a phase I/II study of recombinant IL-6 in human cancer patients, anemia, markedly elevated CRP, and thrombocytosis were observed.[16]

Classic IL-6 signaling involves the binding of IL-6 to the α-subunit of the membrane-bound IL-6 receptor.[17,18] The resulting IL-6/IL-6R complex activates a signal-transducing homodimer of the glycoprotein 130 (gp130) receptor chain, initiating downstream signaling pathways, such as JAK–STAT.[19] In contrast, IL-6 trans-signaling involves the formation of complexes between IL-6 and soluble IL-6 receptor (sIL-6R),

which subsequently activate membrane-bound gp130. All cells in the human body express gp130, whereas IL-6R is only expressed in hepatocytes, some epithelial cells, and some leukocytes.[17] Therefore, IL-6 trans-signaling drastically enlarges the spectrum of IL-6 target cells. IL-6 trans-signaling has emerged as the predominant mechanism promoting IL-6-mediated disease pathogenesis.[17]

Double-transgenic mice that co-express IL-6 and sIL-6R exhibit progressive extramedullary expansion of hematopoietic progenitor cells in the liver and spleen.[20,21] Similarly, splenic extramedullary hematopoiesis (EMH) and plasmacytosis is also observed in transgenic viral IL-6 (vIL-6) murine models of MCD.[19] It should be noted that vIL-6, in contrast to human IL-6, does not require the IL-6R to stimulate target cells. Therefore, vIL-6 does not require sIL-6R and, reminiscent of IL-6 trans-signaling, can stimulate all cells in the human body.[22] Taken together, these findings suggest that IL-6 trans-signaling (by IL-6 and sIL-6R) and subsequent hyperactivation of gp130 may serve as a driver of EMH. Despite these observations in animal studies and the IL-6-driven pathogenesis, EMH has yet to be described in human cases of iMCD. The objective of this case series is to evaluate clinical, laboratory, and radiological data from four iMCD patients exhibiting EMH to assist in clinical recognition and decision making involving this heterogeneous disease and its various subtypes moving forward.

2 | METHODS

Reporting of case 1 was approved by the Dalhousie Faculty of Medicine Research Ethics Board, with written consent from the patient. All patients in cases 2–4 provided informed consent and the ACCELERATE natural history registry has received ethical approval from the University of Pennsylvania institutional review board, with most recent approval on 11 July 2024 (Protocol: 824758).

We identified a 24-year-old female with a challenging diagnosis of CD presenting with fever, elevated CRP, mixed features of TAFRO (small lymphadenopathy, fibrosis, severe thrombocytopenia) and iMCD-NOS (no anasarca, normal renal function) who had EMH in her core lymph node biopsy at Dalhousie University, Halifax, Nova Scotia. We then interrogated the ACCELERATE (Advancing Castleman Care with an Electronic Longitudinal Registry, E-Repository, and Treatment Effectiveness research) database and identified three additional cases of EMH in CD.[23] ACCELERATE is a natural history registry established in 2016 to understand the natural history, pathogenesis, and real-world treatment responses of CD by collecting clinical, laboratory, and outcome data on patients.[23] ACCELERATE uses a two-arm approach, consisting of a patient-powered and a physician-directed arm.[23] Each CD case enrolled in the database receives a thorough review and grade from a panel of expert hematopathologists on the Certification and Access Subcommittee (CAS) to ensure optimal CD cases are included for analyses and publications.[23] Clinical, laboratory, and radiological data were extracted. Scanned images of histology from the ACCELERATE database were examined for EMH.

3 | RESULTS

Baseline clinical and laboratory characteristics of the four patients are summarized in Tables 1 and 2, respectively.

3.1 | Case 1

A previously healthy 24-year-old white female presented to her local emergency department with a two-week history of gingival swelling and bleeding, heavy menstrual bleeding, and 2 days of nausea, vomiting, fatigue, and fever (38.3°C; Table 1). Bloodwork revealed severe anemia (Hb: 6.4 g/dL), thrombocytopenia (platelets: 11×10^3/μL), elevated CRP (91.3 mg/L), and polyclonal hypergammaglobulinemia with elevated IgG (2407 mg/dL; Table 2). A Positron Emission Tomography/Computed Tomography (PET/CT) body scan revealed hepatosplenomegaly (liver: unspecified; spleen: 13.9 cm) and multiple small but enlarged lymph nodes above and below the diaphragm in the left supraclavicular, left inguinal, left common iliac, paraaortic, and bilateral axillary, retropectoral, and external iliac regions (Figure 1A, B). The largest lymph node was 3.5 × 2.6 cm, along the proximal left common iliac chain, had a high standardized uptake value (SUV) max of 20.7 and a liver/tumor ratio of 5 (Table 1).

A bone marrow biopsy revealed hypercellular bone marrow (90% cellularity) with grade MF-2 (of 3, WHO 2016) reticulin fibrosis, increased polytypic plasma cells (5%–8%), a few lymphoid aggregates, and nondysplastic megakaryocytic hyperplasia with rare emperipolesis (Figure 2). The patient exhibited a 46, XX karyotype and was negative for JAK2 V617F. Trichrome staining did not show significant collagen deposition, and flow cytometry showed no phenotypically abnormal hematologic population.

The needle core biopsies of the left inguinal lymph node showed predominantly small, regressed follicles. The interfollicular space was populated by mature lymphocytes, histiocytes, a prominent plasma cell population, and demonstrated high endothelial vessel proliferation and open sinuses (Figure 3A) consistent with a mixed form of CD. Notably, numerous megakaryocytes were identified, consistent with EMH (Figure 3B). Immunohistochemical (IHC) studies confirmed the reactive nature of the germinal centers (positive for CD20, BCL6, and negative for BCL2). The interfollicular areas showed a T-cell predominance (CD3 and CD5-positive) without an abnormal immunophenotype. Plasma cells were polytypic. In situ hybridization for EBER and immunohistochemistry for CMV and HHV-8 were negative. HIV testing was negative. Special stains (Periodic acid-Schiff stain [PAS], Acid Fast Bacteria, Steiner stain) failed to identify microorganisms. Additional BRAF, factor XIIA, CD68, S100 staining was negative ruling out histiocyte disorders such as Erdheim-Chester disease and Rosai-Dorfman-Destombes disease.

The diagnosis of TAFRO was entertained given her diffuse lymphadenopathy, hepatosplenomegaly, elevated inflammatory markers, severe thrombocytopenia, fibrosis, and megakaryocyte hyperplasia. However, given the absence of anasarca and renal dysfunction, she was diagnosed with iMCD-NOS. She was treated initially with

TABLE 1 Patient clinical presentations.

	Patient 1	Patient 2	Patient 3	Patient 4
Demographic information				
Sex	Female	Male	Male	Male
Age at diagnosis	24	23	20	50
Race	White	Asian	White	White
Clinical characteristics				
Clinical Summary	Presented to ED with gingival bleeding, fever, and pancytopenia	Presented to ED with decreased appetite, fatigue, diarrhea, fevers, cherry hemangiomas, and edema	Presented to ED with shortness of breath, fevers, cough, chills, and diarrhea	Presented to ED with swelling in legs, drenching night sweats, fever, weight loss, and palpable inguinal LAD
Constitutional Sx	Present	Present	Present	Present
Fatigue	Present	Present	Present	Present
Night sweats	Not Present	Not Present	Not Present	Present
Fever	Present	Present	Present	Present
Weight loss	Not Present	Not Present	NA	Present
Organomegaly	Present	Present	Present	Present
Hepatomegaly	Present	Not Present	Present	Not Present
Splenomegaly	Present	Present	Present	Present
CD Skin Disorder	Not Present	Present	Not Present	Not Present
Lymphocytic Interstitial Pneumonia (LIP)	Not Present	Not Present	NA	Not Present
Fluid Retention	Not Present	Present	Present	Present
Proteinuria	Trace	Present	NA	Present
Radiologic findings				
Stations of LAD	• Left Supraclavicular • B/L Axillary • B/L Retropectoral • Paraaortic • Aortocaval • B/L External Iliac • Left Inguinal • Left Common Iliac	• B/L Cervical • B/L Axillary • Mediastinal • Paraaortic • Mesenteric • B/L Inguinal • B/L Internal Iliac	• Left Axillary • Left Hilar • Paraaortic • B/L Inguinal • B/L Internal Iliac	• B/L Inguinal • B/L Internal Iliac • B/L External Iliac
Largest LN	Left Common Iliac: 3.5 × 2.6 cm	Left Axillary: 2.8 cm (short axis)	Paraaortic: 4.0 cm (long axis)	Right Inguinal: 3.4 × 1.7 cm
Highest FDG	Left Common Iliac: 20.7 SUV	Right Axillary: 2.3 SUV	Paraaortic: 8.7 SUV	Left External Iliac: 4.9 SUV
Liver Size	Unspecified, Enlarged	Unspecified, Nonenlarged	21.0 cm	"Mild Hepatomegaly"
Spleen Size	13.9 cm	17.3 cm	16.0 cm	16.9 cm

Abbreviations: CD, Castleman Disease; ED, Emergency Department; LAD, Lymphadenopathy; LN, Lymph Node.

dexamethasone, which improved her platelet count and CRP to 108 giga/L and 12.4 mg/L respectively. She subsequently received siltuximab 11 mg/kg intravenously every 3 weeks, which produced complete clinical, biochemical, and radiological responses and allowed her to taper off dexamethasone (Supplemental Table S1). Repeat PET-CT scan showed resolution of her lymphadenopathy and splenomegaly after 6 weeks of siltuximab treatment (Figure 1C).

3.2 | Case 2

A 23-year-old Asian (Sri-Lankan) male with no significant past medical history presented with decreased appetite, fatigue, diarrhea, fevers, cherry hemangiomas, and edema. Labs revealed anemia (Hb: 6.1 g/dL), thrombocytopenia (platelets: $21 \times 10^3/\mu L$), elevated CRP (271.1 mg/L), hypoalbuminemia (15 g/L), reduced estimated glomerular filtration rate

TABLE 2 Laboratory values at baseline ($+/-$ 90 days from diagnosis).

Laboratory Markers	Patient 1	Patient 2	Patient 3	Patient 4
CRP (mg/L; ref ≤10.0)	91.3 ↑	271.1 ↑↑	362.0 ↑↑	NA
Hemoglobin (g/dL; ref >12.5 [Male], >11.5 [Female])	6.4 ↓↓	6.1 ↓↓	7.6 ↓↓	9.4 ↓
Platelets (10^3/μL; ref 150–400)	11 ↓↓	21 ↓↓	21 ↓↓	44 ↓↓
Albumin (g/dL; ref >3.5)	3.6	1.5 ↓↓	1.9 ↓↓	2.3 ↓↓
IgG (mg/dL; ref <1700)	2407 ↑	1512	662	NA
IgA (mg/dL; ref 90–350)	408 ↑	407 ↑	126	NA
Gammaglobulin (g/dL; ref <1.7)	2.37 ↑	1.5	0.66	NA
WBC (10^3/μL; ref 4.5–11.0)	0.9 ↓	25.7 ↑↑	41.9 ↑↑	13.7 ↑
ANC (10^3/μL; ref 1.7–7.0 k/uL)	NA	23.95 ↑↑	38.5 ↑↑	9.1 ↑
ALP (IU/L; ref 44–147)	125	245 ↑	1101 ↑↑	190 ↑
Ferritin (ng/mL; ref 12–300 [Male], 12–150 [Female])	3779.8 ↑↑↑	245	NA	NA
Fibrinogen (mg/dL; ref 200–400)	510 ↑	562 ↑	620 ↑	NA
D-Dimer (ug/mL; ref <0.5 ug/mL [FEU]; <0.25 [DDU])	2.631 ↑↑	NA	8 (FEU) ↑	NA
INR (unitless; ref 0.8–1.1)	1.0	1.5 ↑	1.8 ↑	1.32 ↑
PTT (seconds; ref 25–35)	26	43.2 ↑	51 ↑	33.3 ↑
Total Bilirubin (mg/dL; ref 0.3–1.9)	0.58	2.9 ↑	2.5 ↑	0.8
MCV (fL; ref 80–100)	NA	63 ↓	100.1 ↑	78.8 ↓
Creatinine (mg/dL; ref 0.7–1.3 [Male], 0.6–1.1 [Female])	0.80	7.25 ↑↑↑	2.6 ↑↑	1.43 ↑
eGFR (mL/min/1.73 m^2; ref >60)	NA	9 ↓↓↓	60	56

Note: Bolded values indicate laboratory values outside of the normal reference range.

FIGURE 1 Representative images from PET/CT scans performed at diagnosis (A and B), and 2 months later following treatment (C). Figures A (Maximum Intensity Projection) and B (fused coronal PET/CT) demonstrate intensely FDG-avid lymphadenopathy in the left supraclavicular region, bilateral axillae, paraaortic and iliac regions, and left inguinal region. There is also homogenously increased activity through the enlarged spleen and bone marrow. Figure C demonstrates near-complete metabolic resolution of these findings, with new uptake in the left lung (favored to represent pneumonia) and stomach (favored to represent benign inflammation).

(eGFR; 9 mL/min/1.73 m^2), leukocytosis (25.7×10^3/μL) and increased alkaline phosphatase (ALP: 245 IU/L), total bilirubin (2.9 mg/dL), and creatinine (7.25 mg/dL; Table 2). CT revealed ascites/anasarca/pleural effusions, splenomegaly (17.3 cm), and diffuse lymphadenopathy above and below the diaphragm in the mediastinal, paraaortic, mesenteric, and bilateral cervical, axillary, inguinal, and internal iliac regions. The largest lymph node, measuring 2.3 cm (short axis), was located in the left axillary region, and exhibited an SUV max of 2.3 (Table 1). Polymerase chain reaction (PCR) testing for EBV, CMV, HIV, and HSV were all negative.

A bone marrow biopsy revealed mildly hypercellular marrow (>90% cellularity) with myeloid and megakaryocytic hyperplasia with
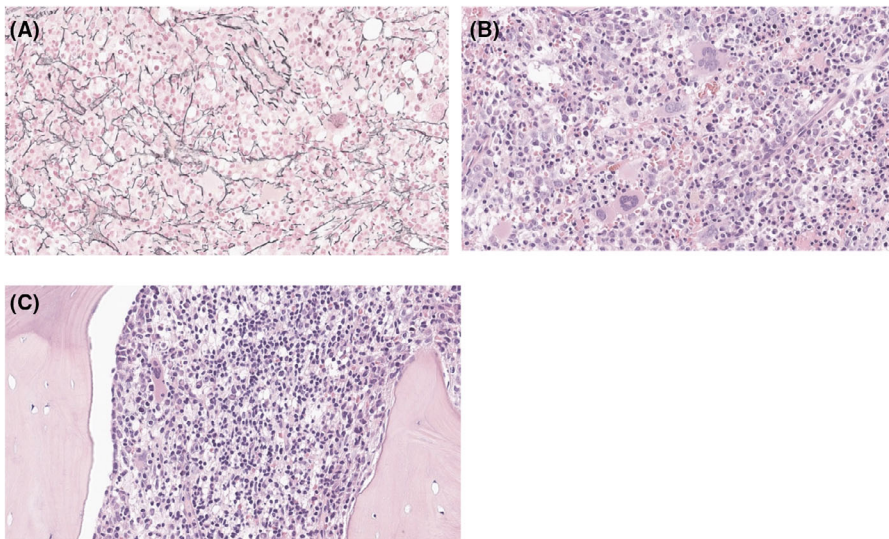
FIGURE 2 Bone marrow biopsy from patient 1. (A). Reticulin stain demonstrates increased reticulin fibrosis with numerous intersections and moderately thick bundles (WHO grade MF-2 of 3). (B) Markedly hypercellular marrow with a preserved myeloid to erythroid ratio. There is megakaryocytic hyperplasia without clustering or dysplastic cytomorphology. Plasma cells are increased and were polytypic by kappa and lambda immunohistochemical stains. (C) Rare megakaryocyte emperipolesis was identified, a nonspecific but characteristic finding in cases of iMCD-TAFRO.
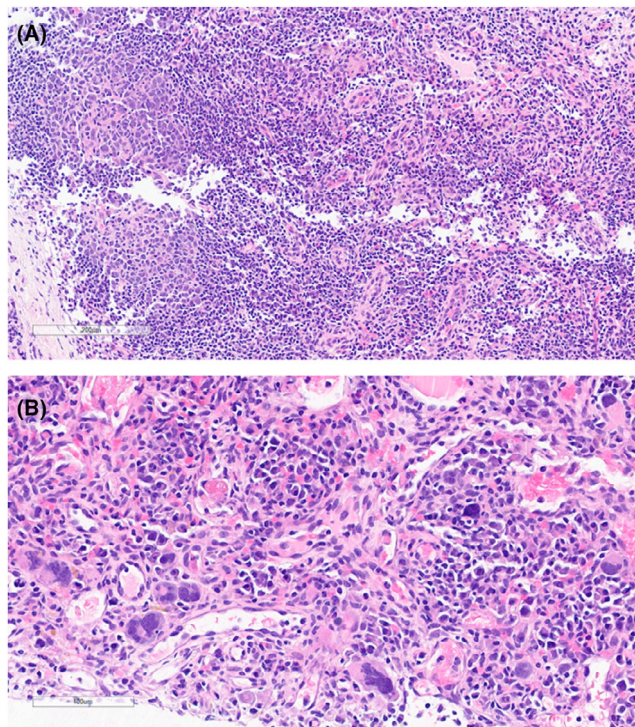

FIGURE 3 Core biopsy of the left inguinal lymph node from patient 1. (A) Two small regressed reactive germinal centers. The parafollicular area shows mature lymphocytes, scattered immunoblasts, occasional plasma cells and notable high endothelial vessel proliferation. (B) Numerous megakaryocytes noted, consistent with extramedullary hematopoiesis.

no increase in blasts or lymphocytes by morphology or flow cytometry. Megakaryocytes exhibited a range or morphologies with large hyperchromatic nuclei which were likely reactive in nature.

An excisional biopsy of the enlarged left axillary lymph node revealed a mixed CD histological subtype consisting of prominent interfollicular vascular hyperplasia with hyalinized blood vessels penetrating germinal centers encircled by concentric rings of mantle zone lymphocytes ("onion skin pattern"). Notably, there were occasional

megakaryocytes present, consistent with EMH. No large abnormal lymphoid cells were identified. IHC stains demonstrated that there were abundant small follicles comprised of CD20+ B-cells scattered throughout the entire lymph node and not confined to the cortex. Interfollicular and paracortical clusters of CD3+ T-cells were also identified. CD138+ polytypic (kappa and lambda chain) plasma cells were abundant in interfollicular areas of the lymph node. Ziehl-Nielsen, Grocott's methenamine silver stain (GMS), and Acid-fast bacteria (AFB) stains were negative for microorganisms. Flow cytometry (FI3-I 191) showed polytypic B-cells, plasma cells, and a mix of T-cell subsets. Histologically, all of these features are characteristic of the HV variant of CD. However, the presence of abundant polytypic plasma cells in the interfollicular areas, systemic lymphadenopathy and B-symptoms are more typically associated with the PC variant of CD. Thus, this case is best considered as a mixed form of CD with features of both HV and PC variants. Hypoalbuminemia and renal failure may be related to his CD. The patient met iMCD-TAFRO criteria (Supplemental Table S2), with multicentric lymphadenopathy above and below the diaphragm, thrombocytopenia (21×10^3/μL), anasarca, fever/elevated CRP (271.1 mg/L), renal dysfunction (mild myelofibrosis on bone marrow biopsy, creatinine: 7.25 mg/dL, and eGFR: 9 mL/min/1.73m^2), and splenomegaly.

Treatment regimen 1, consisting of steroids, anti-CD-20 antibodies (rituximab), and the IL-6R inhibitor (tocilizumab), was initiated, leading to a complete clinical and partial lymph node response following a 5-month regimen. However, 7 years after discontinuing the regimen, he experienced a severe relapse. He was then treated with a tocilizumab and corticosteroid-based regimen, with which he achieved a complete and durable response (see Supplemental Table S1 for detailed patient treatment course).

3.3 | Case 3

A previously healthy 20-year-old white male presented with shortness of breath, fevers, cough, chills, diarrhea, and was admitted to the

intensive care unit (ICU) after he was found to be hypotensive, hypoxic, and tachypneic. Bloodwork revealed anemia (Hb: 7.6 g/dL), thrombocytopenia (platelets: $21 \times 10^3/\mu$L), elevated CRP (362 mg/L), hypoalbuminemia (19 g/L), leukocytosis (WBC: $41.9 \times 10^3/\mu$L), and elevated ALP (1101 IU/L), fibrinogen (620 mg/dL), D-dimer (8 μg/mL FEU), bilirubin (2.5 mg/dL), and creatinine (2.6 mg/dL; Table 2). CT scan revealed significant anasarca, reticulin fibrosis, and hepatosplenomegaly (liver: 21.0 cm; spleen: 16.0 cm; Table 1). CT also revealed diffuse lymphadenopathy in the neck, left axillary, left hilar, paraaortic, and bilateral inguinal, and internal iliac regions. The largest lymph node, measuring 4.0 cm (long axis), was located in the paraaortic region, and exhibited an SUV max of 8.7 (Table 1). He later developed respiratory and kidney failure which required intubation, mechanical ventilation, and hemodialysis. Laboratory testing revealed IL-6 levels >1000 (normal range: <3.7 pg/mL).

Cervical lymph node biopsies showed regressed follicles with surrounding plasma cell aggregates and vascular hyperplasia and were classified as HV CD histologically. CD3 and CD20 stains showed adequate T- and B-cells. Plasma cells were shown to be polyclonal for kappa and lambda light chains. Staining for HHV8 was negative. Brown & Brenn, GMS, and AFB staining were all negative for microorganisms. HIV testing was negative.

Histological sections of the spleen showed prominent vascular congestion and scattered megakaryocytes within the red pulp, indicative of splenic EMH. There was also prominent plasmacytosis within the white pulp. A bone marrow biopsy showed maturing megakaryocytic hyperplasia, mildly hyperplastic marrow, mildly increased reticulin fibers, no significant dysgranulopoiesis or dyserythropoiesis, and unremarkable flow cytometric studies.

The patient met iMCD-TAFRO criteria (Supplemental Table S2), with multicentric lymphadenopathy above and below the diaphragm, thrombocytopenia ($21 \times 10^3/\mu$L), anasarca, fever/elevated CRP (CRP: 362 mg/L), renal dysfunction (creatinine: 2.6 mg/dL, eGFR: 60 mL/min/1.73m^2), and splenomegaly.

He was initiated on steroids and plasmapheresis (regimen 1), followed by anti-CD-20 therapy (rituximab; regimen 2) after experiencing a flare-up 3 years later, which provided a partial clinical response. He was then enrolled in phase 2 of the siltuximab (anti-IL-6) clinical trial (regimen 3) which resulted in a complete clinical and lymph node response which the patient remains on to present day (see Supplemental Table S1 for full patient treatment course).

3.4 | Case 4

A 50-year-old white male with a past medical history of neutropenia and microcytosis (5 months prior) presented with swelling in the legs, drenching night sweats, fever, weight loss, and palpable inguinal lymphadenopathy. Labs revealed anemia (Hb: 9.4 g/dL), thrombocytopenia (platelets: $44 \times 10^3/\mu$L), hypoalbuminemia (23 g/L), leukocytosis ($13.7 \times 10^3/\mu$L), elevated ALP (190 IU/L), elevated creatinine (1.43 mg/dL), and reduced eGFR (56 mL/min/1.73 m^2; Table 2). A CT scan revealed mild hepatomegaly, splenomegaly (16.9 cm), and

enlarged lymph nodes in bilateral inguinal, internal iliac, and external iliac regions (Table 1). The largest lymph node, measuring 3.4 cm × 1.7 cm, was located along the left external iliac chain and exhibited an SUV max of 4.9.

An excisional biopsy of a right inguinal lymph node was performed and showed abnormal architecture comprised of follicular centers, some of which were in various stages of regression coupled with expanded interfollicular components, consistent with the HV subtype of CD. Interfollicular areas showed a heterogenous cell population comprised of small lymphocytes, plasma cells, and occasional histiocytes. In addition, very prominent vascular proliferation was evident in the expanded stromal areas. Sclerotic penetrating vessels were also identified in some of the germinal centers forming so-called "lollipop lesions." Megakaryocytes were present and indicated EMH (Supplemental Figure S1). No significant eosinophilia was identified. HHV-8 and HIV testing was negative. Notably, the patient has a mutation in the KRAS gene (Ki-rast2 Kirsten rat sarcoma vial oncogene homolog).

Ultimately, the patient met iMCD-TAFRO criteria (Supplemental Table S2) with multicentric lymphadenopathy, thrombocytopenia, anasarca, fever, renal dysfunction, and hepatosplenomegaly. He was initiated on steroids alongside a combination of IL-6 inhibitors in a number of complex regimens (12 total) prior to achieving a complete clinical response (see Supplemental Table S1 for complete treatment course). Despite 4 years of continuous treatment, he still experiences persistent leg swelling, bone pain, and abdominal pain.

4 | DISCUSSION

This case series demonstrates that EMH, characterized by megakaryocyte hyperplasia and peripheral blood thrombocytopenia, can be seen in a subset of patients with iMCD. Although EMH has been previously reported in murine models of CD, likely through hyper-activation of gp130 via IL-6 trans-signaling, this case series is the first of its kind to describe lymph node and splenic EMH in human cases of MCD.[19,24]

EMH on lymph node biopsy may serve as an important clue in the diagnosis of iMCD. The differential diagnosis of various subtypes of CD is broad and particularly challenging. iMCD-TAFRO patients are typically very ill with severe cytokine storm and the involved lymph nodes are small volume, and the yield of needle or even excisional biopsies is lower than in patients with large peripheral lymphadenopathy in iMCD-NOS. In this case series, patient 1 met two of the three major clinical criteria (thrombocytopenia, systemic inflammation) and three minor criteria (Castleman disease-like features on lymph node biopsy, bone marrow biopsy showing reticulin fibrosis, and mild organomegaly) of iMCD-TAFRO. Patients 2–4 fulfilled all three major and four minor clinical criteria of iMCD-TAFRO. All four patients had severe thrombocytopenia, inflammation, reticulin fibrosis, and small, diffuse lymphadenopathy.[25]

In animal models, EMH and plasma cell hyperplasia in the spleen and liver were reported to be IL-6 dependent proliferative responses associated with a Castleman-disease-like illness in mouse models, as

demonstrated by Rose-John et al.[19,21] In an additional mouse model, mice transgenic for vIL-6 developed key features of human plasma cell-type MCD including splenomegaly, multifocal lymphadenopathy, hypergammaglobulinemia, and plasmacytosis. Strikingly, endogenous IL-6 was needed to develop this phenotype since breeding vIL-6 transgenic mice on an IL-6 deficient background abrogated the MCD-like phenotype.[19]

In other diseases commonly associated with EMH, such as thalassemia major and hereditary spherocytosis, erythroid islands as well as megakaryocytes are often seen.[26,27] In contrast, EMH in this case series features megakaryocytes most prominently, and to a lesser extent, granulopoiesis. IL-6 is known to stimulate granulopoiesis and megakaryocyte production and maturation,[28] whereas IL-6 inhibits erythropoiesis.[29]

Another distinctive feature of case 1 in this series is the high SUV max of 20. Castleman's lymphadenopathy typically displays moderate FDG avidity, with an SUV max ranging from 1.6–11.5 in other studies.[30] However, this image was taken on a new PET scanner at Dalhousie University which is more sensitive than older scanners. Importantly, the tumor-to-liver (T/L) ratio was 5 which is within 2 standard deviations of most subtypes of CD.[30]

This small case series should be viewed as a hypothesis-generating study. Because of the retrospective nature of the data collection for cases 2–4 we were not able to obtain publication-quality images of the EMH described in the reports for these patients. The novel finding of EMH in human CD, when viewed in the context of established EMH in animal models of CD, raises a number of interesting questions for further study. Although EMH could be related to elevated IL-6 in humans, the findings outlined in this report were observed in a small number of cases and have limited generalizability at this time. Further work is needed to ascertain the cause of EMH in CD. Castleman disease encompasses a wide variety of clinical syndromes with a wide variety of clinical and laboratory features ranging from UCD to iMCD-NOS to iMCD-TAFRO. The unifying characteristic of all these disorders is characteristic histology of CD in lymph nodes, which is further subdivided into plasmacytic, hypervascular, or mixed. The observation of EMH in CD raises the question of how much the LN morphology of CD represents a unifying pathophysiology and how much is a result of cytokine-mediated changes in hemato-lymphatic tissues.

In conclusion, extramedullary hematopoiesis is present in a subset of human patients with iMCD with overt TAFRO or TAFRO-like features. This extends the finding of EMH in mouse models of CD and invites further research into the pathophysiology of Castleman-like changes in lymph nodes.

AUTHOR CONTRIBUTIONS

All authors participated and contributed equally to study design, data collection and analysis, and writing and editing of the manuscript.

CONFLICT OF INTEREST STATEMENT

D.C.F. has received research funding for the ACCELERATE registry from EUSA Pharma and consulting fees from EUSA Pharmac, and Pfizer has provided a study drug with no associated research funding for the clinical trial of sirolimus (NCT03933904). D.C.F. has two provisional patents pending related to the diagnosis and treatment of iMCD.

DATA AVAILABILITY STATEMENT

The data that support the findings of this study are available on request from the corresponding author, LC.

ORCID

Stefan Rose-John 🆔 https://orcid.org/0000-0002-7519-3279
Luke Y. C. Chen 🆔 https://orcid.org/0000-0002-9551-2951

REFERENCES

1. Fajgenbaum DC, Uldrick TS, Bagg A, et al. International, evidence-based consensus diagnostic criteria for HHV-8-negative/idiopathic multicentric Castleman disease. *Blood*. 2017;129(12):1646-1657.
2. Chen L, Fajgenbaum DC. Castleman disease. In: Stone JH, ed. *A Clinician's Pearls & Myths in Rheumatology*. Springer International Publishing; 2023:727-735.
3. Henrie R, Cherniawsky H, Marcon K, et al. Inflammatory diseases in hematology: a review. *Am J Physiol Cell Physiol*. 2022;323(4):C1121-C1136.
4. Nishikori A, Nishimura MF, Fajgenbaum DC, et al. Diagnostic challenges of the idiopathic plasmacytic lymphadenopathy (IPL) subtype of idiopathic multicentric Castleman disease (iMCD): factors to differentiate from IgG4-related disease. *J Clin Pathol*. 2024;jcp-2023-209280.
5. González García A, Fernández-Martín J, Robles Marhuenda Á. Idiopathic multicentric Castleman disease and associated autoimmune and autoinflammatory conditions: practical guidance for diagnosis. *Rheumatology*. 2023;62(4):1426-1435.
6. Chen LYC, Skinnider BF, Wilson D, Fajgenbaum DC. Adrenalitis and anasarca in idiopathic multicentric Castleman's disease. *Lancet*. 2021;397(10286):1749.
7. Masaki Y, Arita K, Sakai T, Takai K, Aoki S, Kawabata H. Castleman disease and TAFRO syndrome. *Ann Hematol*. 2022;101(3):485-490.
8. Zhao EJ, Cheng CV, Mattman A, Chen LYC. Polyclonal hypergammaglobulinaemia: assessment, clinical interpretation, and management. *Lancet Haematol*. 2021;8(5):e365-e375.
9. Festen C, Flendrig JA, Schillings PH. Giant lymphomas. *Ned Tijdschr Geneeskd*. 1969;113(43):1918-1919.
10. Keller AR, Hochholzer L, Castleman B. Hyaline-vascular and plasma-cell types of giant lymph node hyperplasia of the mediastinum and other locations. *Cancer*. 1972;29(3):670-683.

11. Nguyen D, Diamond L, Hansmann M, et al. Castleman's disease. Differences in follicular dendritic network in the hyaline vascular and plasma cell variants. *Histopathology*. 1994;24(5):437-443.

12. Radaszkiewicz T, Hansmann ML, Lennert K. Monoclonality and polyclonality of plasma cells in Castleman's disease of the plasma cell variant. *Histopathology*. 1989;14(1):11-24.

13. Dispenzieri A, Fajgenbaum DC. Overview of Castleman disease. *Blood*. 2020;135(16):1353-1364.

14. Fajgenbaum DC, van Rhee F, Nabel CS. HHV-8-negative, idiopathic multicentric Castleman disease: novel insights into biology, pathogenesis, and therapy. *Blood*. 2014;123(19):2924-2933.

15. Brandt SJ, Bodine DM, Dunbar CE, Nienhuis AW. Dysregulated interleukin 6 expression produces a syndrome resembling Castleman's disease in mice. *J Clin Invest*. 1990;86(2):592-599.

16. van Gameren MM, Willemse PH, Mulder NH, et al. Effects of recombinant human interleukin-6 in cancer patients: a phase I-II study. *Blood*. 1994;84(5):1434-1441.

17. Rose-John S, Jenkins BJ, Garbers C, Moll JM, Scheller J. Targeting IL-6 trans-signalling: past, present and future prospects. *Nat Rev Immunol*. 2023;23(10):666-681.

18. Chen LYC, Biggs CM, Jamal S, Stukas S, Wellington CL, Sekhon MS. Soluble interleukin-6 receptor in the COVID-19 cytokine storm syndrome. *Cell Rep Med*. 2021;2(5):100269.

19. Suthaus J, Stuhlmann-Laeisz C, Tompkins VS, et al. HHV-8-encoded viral IL-6 collaborates with mouse IL-6 in the development of multicentric Castleman disease in mice. *Blood*. 2012;119(22):5173-5181.

20. Peters M, Schirmacher P, Goldschmitt J, et al. Extramedullary expansion of hematopoietic progenitor cells in interleukin (IL)-6–sIL-6R double transgenic mice. *J Exp Med*. 1997;185(4):755-766.

21. Schirmacher P, Peters M, Ciliberto G, et al. Hepatocellular hyperplasia, plasmacytoma formation, and extramedullary hematopoiesis in interleukin (IL)-6/soluble IL-6 receptor double-transgenic mice. *Am J Pathol*. 1998;153(2):639-648.

22. Müllberg J, Geib T, Jostock T, et al. IL-6 receptor independent stimulation of human gp130 by viral IL-61 *J Immunol*. 2000;164(9):4672-4677.

23. Pierson SK, Khor JS, Ziglar J, et al. ACCELERATE: a patient-powered natural history study design enabling clinical and therapeutic discoveries in a rare disorder. *Cell Rep Med*. 2020;1(9):100158.

24. Kallen KJ. The role of transsignalling via the agonistic soluble IL-6 receptor in human diseases. *Biochim Biophys Acta*. 2002;1592(3):323-343.

25. Iwaki N, Fajgenbaum DC, Nabel CS, et al. Clinicopathologic analysis of TAFRO syndrome demonstrates a distinct subtype of HHV-8-negative multicentric Castleman disease. *Am J Hematol*. 2016;91(2):220-226.

26. Molina-Urra R, Martinez D, Sagasta A, et al. Paraspinal extramedullary hematopoiesis in hereditary spherocytosis with a concurrent follicular lymphoma: case report and review of the literature. *Diagn Pathol*. 2015;10(1):158.

27. Subahi EA, Ata F, Choudry H, et al. Extramedullary haematopoiesis in patients with transfusion dependent beta-thalassaemia (TDT): a systematic review. *Ann Med*. 2022;54(1):764-774.

28. Navarro S, Debili N, Le Couedic JP, et al. Interleukin-6 and its receptor are expressed by human megakaryocytes: in vitro effects on proliferation and endoreplication. *Blood*. 1991;77(3):461-471.

29. Andrews NC. Anemia of inflammation: the cytokine-hepcidin link. *J Clin Invest*. 2004;113(9):1251-1253.

30. Han EJ, O JH, Jung SE, et al. FDG PET/CT findings of Castleman disease assessed by histologic subtypes and compared with laboratory findings. *Diagnostics (Basel)*. 2020;10(12):1-8.

SUPPORTING INFORMATION

Additional supporting information can be found online in the Supporting Information section at the end of this article.